Physicochem. Probl. Miner. Process., 59(6), 2023, 172481

http://www.journalssystem.com/ppmp

Physicochemical Problems of Mineral Processing

ISSN 1643-1049

Insights into the depression effect and adsorption mechanism of HACC on chalcopyrite surface in Cu-Mo flotation separation

Mingyang Li [1,2], Pengpeng Zhang [2], Xiangpeng Gao [2], Lingyun Huang [1]

[1] State Key Laboratory of Complex Nonferrous Metal Resources Clean Utilization, Kunming 650093, China

[2] School of Metallurgical Engineering, Anhui University of Technology, Ma'anshan 243002, China

Corresponding author: 12607199@qq.com (Lingyun Huang)

Abstract: In this study, hydroxypropyltrimethyl ammonium chloride chitosan (HACC) was first introduced as a depressant during separating chalcopyrite from molybdenite (Cu-Mo). The selective effects of HACC on the separation of Cu-Mo were conducted by single-mineral flotation experiments. The findings from this study revealed that HACC helped separate Cu and Mo efficiently at pH 6 with 8 mg/dm^3 of HACC, resulting in 76.22% and 5.38% of Mo and Cu flotation recovery, respectively. The adsorption mechanism of HACC was investigated via zeta potential, adsorption density, and contact angle measurement along with FT-IR and XPS analyses. The contact angle and adsorption density measurements offer indisputable proof that HACC can adsorb on the surface of chalcopyrite. Furthermore, FT-IR and XPS analyses confirm that N atoms in quaternary ammonium groups of HACC interact with Cu sites on the surface of chalcopyrite. The findings also suggest that HACC adsorbs on the surface without significantly impacting molybdenite. All these results confirm that HACC can be an effective chalcopyrite depressant.

Keywords: chalcopyrite, molybdenite, flotation, adsorption, depressant

1. Introduction

Chalcopyrite and molybdenite, being primary sources of Cu and Mo, account for more than half of Cu and over three-quarters of Mo derived from Cu-Mo porphyry ores on a global level (Bulatovic, 2007; Suyantara et al., 2018). Due to the closely coexisting and similar floatability of chalcopyrite and molybdenite, it is difficult to separate chalcopyrite from molybdenite for Cu-Mo porphyry ores (Ansari & Pawlik, 2007; Triffett et al., 2008). Therefore, efficiently separating chalcopyrite and molybdenite is vital in meeting the high demand for Cu and Mo metal globally.

It is a well-known fact that flotation is one of the most prevalent methods successfully employed to separate various minerals based on their unique floatability (Poperechnikova et al., 2017; Li et al., 2020; Chen et al., 2023; Mao et al., 2023). Due to molybdenite's higher natural floatability than chalcopyrite, chalcopyrite is typically depressed while molybdenite is floated into frother products in the flotation process (Wei et al., 2021). Therefore, a depressant with selective depression on chalcopyrite is vital for the separation of chalcopyrite and molybdenite(Zhong et al., 2021).

For decades, cyanide, sodium sulfide, sodium hydrosulfide, thioglycolate, and Nokes reagents have been the most widely used depressants for chalcopyrite (Yin et al., 2010; Yin et al., 2017; Peng et al., 2017; Yuan et al., 2019; Yan et al, 2020; Chen et al., 2020). However, these reagents come with significant drawbacks, including the excessive toxicity of cyanide and harm to humans and the environment. Then, the production of hydrogen sulfide by sodium sulfide and sodium hydrosulfide into the air brings potential hazards to operators and laborers. These limitations on their usage are primarily caused by the ever-growing environmental protection pressures. In order to deal with these deficiencies, numerous research efforts have been dedicated to discovering innovative Cu depressants to optimize the separation of chalcopyrite and molybdenite. Some of them contain -SH groups, for instance, disodium carboxy methyl trithiocarbonate (DCMT) demonstrated excellent depression for chalcopyrite, with a Cu recovery of 8.72% (Yin et al., 2017). We reported an effective chalcopyrite depressant, 2,3-

DOI: 10.37190/ppmp/172481

disulfanyl butanedioic acid (DMSA) which indicated an optimal depression outcome at pH 6.0, with 95% of chalcopyrite being depressed during mixed mineral flotation separation (Li et al., 2015). Besides that, thio carbono hydrazide (TCH), poly(acrylamide-allylthiourea) (PAM-ATU), and L-cysteine exhibited satisfactory separation performance (Guan et al., 2018; Zhang et al., 2020; Yin et al., 2020). Despite the superior outcomes of these depressants when compared to conventional ones, they have not been widely used in flotation plants because of their expense.

Natural macromolecular organic depressants have the advantages of less dosage, biodegradability, and low cost, and have attracted more and more attention. Zeng et al. (2020) studied the depression effects of sodium alginate (SA) on chalcopyrite and molybdenite during the flotation process. The results of the single mineral flotation experiments suggested that SA can effectively inhibit chalcopyrite. However, the selectivity of SA weakened during artificial mixed ore flotation, which has a significant depression effect on chalcopyrite and molybdenite, mainly because Cu^{2+} and $Cu(OH)^{+}$ will be adsorbed on molybdenite due to electrostatic interaction. The influence of Cu^{2+} and other metal cations in the pulp can be eliminated or weakened by the combination use of SA and kerosene. For the first time, we applied chitosan in Cu-Mo separation and found that the chitosan can selectively depress the flotation of chalcopyrite to a certain extent (Li et al., 2015). Further mechanistic analysis revealed that chitosan adsorbed on chalcopyrite through amino and amide groups, while it adsorbed on molybdenite only through amide groups.

Although chitosan exhibits good selectivity in the separation of chalcopyrite and molybdenite, due to the free hydroxyl and amino groups on the chitosan molecule, hydrogen bonds are easily formed between the molecules, so the chitosan molecule is difficult to dissolve in water, especially when the pH>7 (Rinaudo, 2016). The poor solubility of chitosan severely limits its application range. Therefore, it is necessary to chemically modify it to change its physical and chemical properties, usually by introducing water-soluble groups, introducing bulky hydrocarbon groups to destroy the hydrogen bonds between its crystals, etc. to improve water solubility (Andreica et al., 2020). Quaternary ammonium salt is a modification method that is widely used. The chitosan quaternary ammonium salt prepared by introducing quaternary ammonium salt groups into CTS maintains the original excellent properties of CTS such as biocompatibility and degradability (Liu et al., 2015). At the same time, the water solubility is greatly improved, the working pH range is enlarged, the adsorption sites are increased, and the charge density energy is also enhanced (Ma et al., 2017).

In this study, the capability of hydroxyl propyl trimethyl ammonium chloride chitosan (HACC) for the selective depression of chalcopyrite and molybdenite during the process was thoroughly probed. To comprehend the depression performance of HACC on the surface of chalcopyrite, single-mineral flotation experiments with chalcopyrite and molybdenite minerals were conducted. Furthermore, the adsorptive mechanism of HACC was revealed by zeta potential, contact angle, adsorption density, FT-IR, and XPS measurements.

2. Materials and methods

2.1. Materials

The block-shaped high-quality chalcopyrite and the molybdenite samples were sourced from a mine in Yunnan province, and Jima copper-bearing mine in Tibet, China, respectively. To eliminate minor impurities, the ores were crushed to a -5 mm particle size, and high-quality particles were selected. The samples were then crushed to -0.25 mm and screened using a shake table to increase the purity. Finally, the purified chalcopyrite and the molybdenite samples were dried in a vacuum desiccator at 25°C. The ore was then ground to a -100 μm particle size using a marble mill, and the -100+45 μm size fraction was sieved for single-mineral flotation experiments. The -45 μm particle size fraction samples were then ground to -2 μm for the experimental studies.

The collector kerosene, depressant HACC, frother terpenic oil, pH modifiers HCl and NaOH were sourced from Adamas-beta® (Shanghai Titan Scientific Co. Ltd.), while deionized (DI) water, with a measured resistivity of 18.2 MΩ.cm was utilized in all the experiments.

2.2. Methods

2.2.1. Characterization of materials

The X-ray diffraction (XRD) analysis of the single-mineral samples is shown in Fig. 1. The results indicate that the samples have a high purity and contain almost no other impurity minerals. The chemical element analysis of the single-mineral samples, using Inductively Coupled Plasma (ICP) spectroscopy, further showed that the Cu grade in the chalcopyrite and Mo grade in the molybdenite sample was 32.84% and 54.09%, respectively. The corresponding purities of the samples were 95.02% and 90.24%, respectively. The specific surface areas of the -100+45 μm particle size chalcopyrite and molybdenite samples, measured using an automated adsorption analyzer (Quantachrome, US), were 0.29 m^2/g and 0.56 m^2/g, respectively.

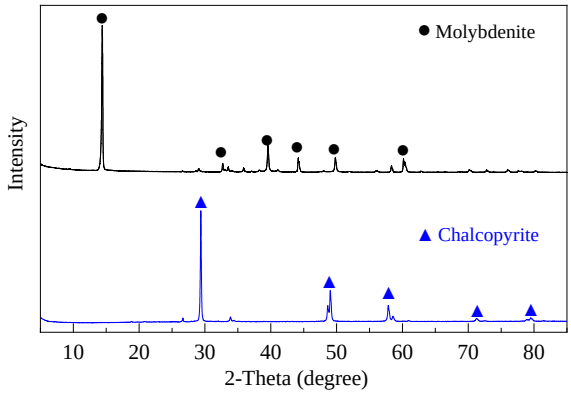

Fig. 1. XRD pattern of chalcopyrite and molybdenite

2.2.2. Flotation experiments

The flotation experiments were carried out in a model XGF-1600 flotation machine (Jilin Exploration Machinery Plant, China) operating at 1600 rpm with a 30 cm^3 suspension cell. For single-mineral flotation experiments, 2 g of the -100+45 μm fraction mineral was positioned into 30 cm^3 of DI water before undergoing ultrasonic cleaning for 5 min to disperse particles and remove the surface oxide layer. Then, either HCl or NaOH solutions were employed to adjust the slurry pH to the preferred value. Next, the HACC solution was added to the slurry and stirred for 3 min. Then, kerosene and terpenic oil were introduced in sequence, functioning as the collector and the frother, and conditioned for 2 min each. After that, the treated slurry was floated for 5 min to harvest the froth products and tailings. Afterward, these materials were dried, weighed, and analyzed to extract the recovery based on the distribution of the solid weight between the froth and tailing fractions. For artificial mixed-mineral flotation, the weight ratio of chalcopyrite and molybdenite was 3:1, and the process was the same as the single-mineral. The grade of each sample of artificially mixed mineral flotation was measured following the Whole Rock Analysis procedure.

2.2.3. Zeta potential measurements

The zeta potential values of the samples were determined using a ZetaPALS potential analyzer (Brookhaven Instruments Ltd. US). In the measurements, 5 mg of mineral sample was mixed, measuring less than 2 μm, into 50 cm^3 of 8 mg/dm^3 HACC solution, with 1×10^{-3} mol/dm^3 KCl acting as a background electrolyte solution, and stirred for 3 min (Luo et al., 2022; Li et al., 2022). Afterward, each sample was adjusted to the specified pH value and homogenized by maintaining it for 2 min. Finally, 1 cm^3 of the suspension was sampled and measured for the zeta potential. The results, including the average values of three independent experiments, were recorded.

2.2.4. Adsorption experiments

Adsorption experiments were performed using TOC-L (Shimadzu Japan) according to the content of total organic carbon (TOC). To determine the quantity of HACC adsorbed by the minerals, the residual

concentration approach was utilized. The samples (2 g) were dispersed uniformly in 30 cm^3 HACC solution (pH=8) for 1 h. Then, the suspensions were sent to a centrifuge before measuring the absorbance of the supernates. The adsorption density of HACC was determined using Eq. (1):

$$\Gamma = \frac{(C_i - C_f)}{S.m} \cdot V \quad (1)$$

where Γ (mg/m^2) is the adsorption density of HACC on minerals, C_i and C_f (mg/dm^3) are the initial and final concentrations of HACC, respectively, V is the volume of solution (dm^3), S (m^2/g) is the BET surface area of the sample, and m is the amount of the sample.

2.2.5. Contact angle measurements

The contact angle of minerals in the solutions was determined using a JC2000A contact angle analyzer (Powereach Instruments, Shanghai, China). The -100+45 μm size fraction chalcopyrite and molybdenite samples were tableted using a mold. Flakes of mineral samples were then placed on the contact angle instrument platform and arranged horizontally before setting the instrument so that the samples were aligned. A program controls the droplets above the mineral sample drops down via an automated sample injection syringe before measuring the contact angle by snapping pictures of the water droplet's profile via a PC. Each contact angle examination was performed at least three times.

2.2.6. Fourier-transform infrared spectroscopy (FT-IR) analysis

A Nicolet 6700 FT-IR spectrometer (Thermo Nicolet Corporation, The United States) was used to record FT-IR spectra within a wave number range from 4000 cm^{-1} to 500 cm^{-1}. The chalcopyrite and molybdenite samples treated with HACC were prepared by following steps. A 2 g sample (< 2 μm) was put into 30 cm^3 HACC solution (8 mg/dm^3) at pH=8. Afterward, the slurry was agitated for 30 min with a magnetic stirrer. In the end, the processed sample was filtered, washed with DI water completely, and air-dried at 30°C for 24 hours.

2.2.7. X-ray photoelectron spectroscopy (XPS) analysis

XPS analyses of the samples were performed by a Thermo ESCALAB 250XI X-ray photoelectron spectrometer (Thermo Fisher Scientific, USA), utilizing an Al Kα monochromatized X-ray source (pass energy of 100 eV, energy step of 1 eV) and collecting survey and high-resolution data simultaneously over a scan range of 1400 eV to 0 eV. C 1s binding energy at 284.6 eV was used for energy calibration. The sample preparation and processing for the XPS analysis were done as mentioned above for FT-IR measurements.

3. Results and discussion

3.1. Flotation experiments

In order to scrutinize the floatability of minerals at various kerosene concentrations and pH levels, single-mineral flotation experiments were conducted in the absence of a depressant. As seen in Fig. 2, the floatabilities of both chalcopyrite and molybdenite increased with the increase of kerosene concentration at pH around 8. Molybdenite showed higher floatability in the concentration range of the collector. Moreover, the floatabilities of the two minerals increased first (pH<8) and then decreased (pH>8) with the increase in pH values. The optimal floatability of the two minerals was achieved with 8 mg/dm^3 kerosene at pH 8, in which the flotation recovery of chalcopyrite and molybdenite reached 85.23% and 91.32%, respectively.

Chalcopyrite and molybdenite show similar floatability with collector kerosene and without a depressant. Therefore, HACC was attempted to depress the float of chalcopyrite selectively, and the recoveries of chalcopyrite and molybdenite at different concentrations and pH values were shown in Fig. 3. It is obvious in Fig. 3a that the addition of HACC strongly depressed the floatability of chalcopyrite, while the depression effect of HACC on molybdenite was much slighter than on chalcopyrite. When the concentration of HACC was 8 mg/dm^3, the flotation recoveries of chalcopyrite and molybdenite were 5.62% and 75.37%, respectively, with a maximum recovery difference of 69.75%.

The pH value of the slurry showed an obscure effect on the floatability of chalcopyrite and molybdenite, as shown in Fig. 3b. The flotation recovery of chalcopyrite increased slightly with the pH increased from 4 to 8, and decreased when pH was over 8. The flotation recovery of molybdenite was hardly affected by the pH of the slurry, in which its recovery stayed under 10% within the whole pH range. As can be seen from the above experiments, the optimum experimental conditions are as follows pH=8, kerosene concentration 8 mg/dm^3, HACC concentration 8 mg/dm^3.

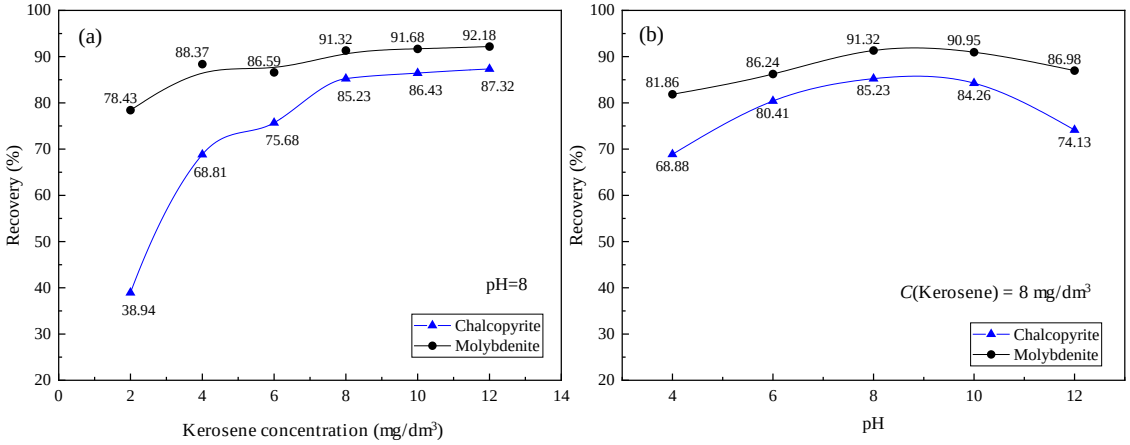

Fig. 2. The recoveries of chalcopyrite and molybdenite as a function of (a) kerosene concentration at pH around 8.0, and (b) pH with 8 mg/dm^3 kerosene without a depressant

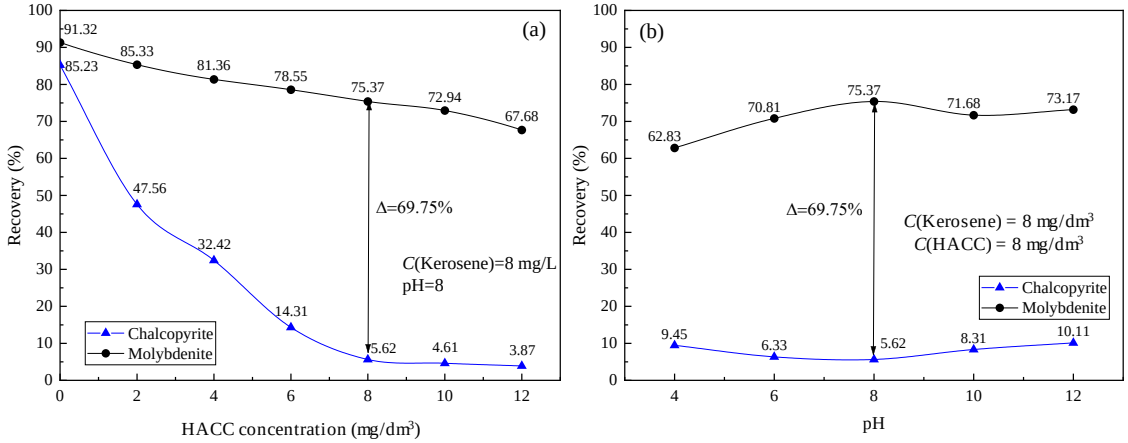

Fig. 3. The recoveries of chalcopyrite and molybdenite as a function of (a) HACC concentration at pH around 8.0, and (b) pH with 8 mg/dm^3 HACC

To further investigate HACC's depression selectivity for chalcopyrite/molybdenite flotation separation, artificial mixed-mineral flotation experiments were carried out. The kerosene concentration was maintained at 8 mg/dm^3 with different HACC concentrations at pH 8, as shown in Fig. 4. The results show that both the recoveries of copper and molybdenum in froth decreased slowly with the increase of HACC concentration. The recoveries of copper and molybdenum declined from about 41% to 9% and 80% to 60% in the HACC concentration range, respectively. The average recovery difference between copper and molybdenum is about 57% in the concentration range of HACC, which indicates that HACC is effective for the separation of chalcopyrite and molybdenite.

3.2. Zeta potential measurements

Figure 5 shows the zeta potentials of untreated and HACC-treated chalcopyrite and molybdenite, as well as their isoelectric points (IEP) determined at roughly pH 5 and 3, which accords with the findings of past literature (Li et al., 2015; Yang et al., 2020). Upon being treated with HACC, the zeta potential of chalcopyrite was elevated (IEP was shifted from 5.11 to 7.47), revealing the probable adsorption of

HACC onto the surface of chalcopyrite. It also has been proved that the N atoms of the triazole ring of HACC were prone to protonation (Al-Manhel et al., 2018). Hence the right shift in zeta potential could be attributed to the uptake of protonated HACC on chalcopyrite surface. When it comes to molybdenite, the positive shift of the zeta potential hardly altered (IEP from 3.42 to 4.81) due to the HACC implementation, denoting that the adherence of HACC species on the molybdenite surface was insignificant.

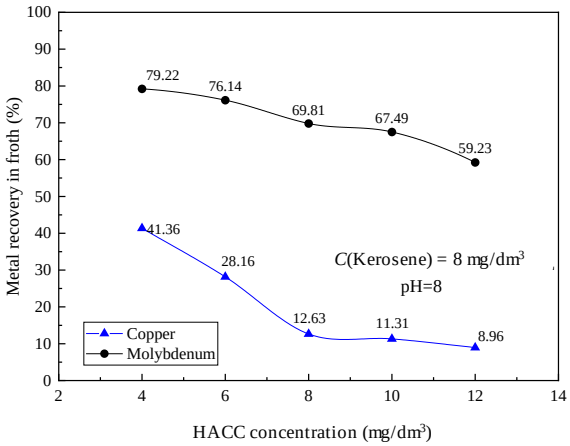

Fig. 4. Recoveries of copper and molybdenum in froth as a function of HACC concentration at pH 8 by collector kerosene (8 mg/dm³)

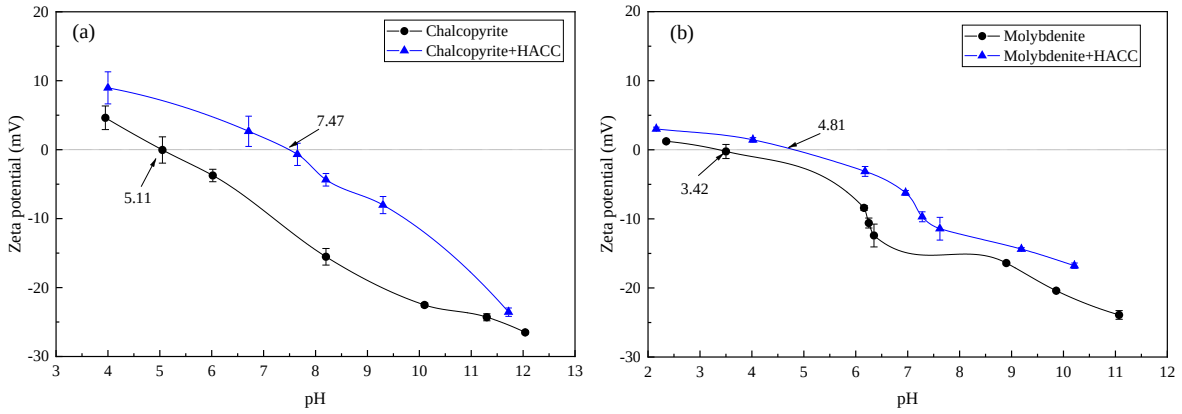

Fig. 5. Zeta potential of (a) chalcopyrite and (b) molybdenite as a function of pH with or without HACC

3.3. Adsorption density measurements

As can be seen in Fig. 6, the adsorption capacity of HACC on chalcopyrite and molybdenite surfaces varies with HACC concentration. The density of HACC adsorbed on chalcopyrite surface grew prominently in accordance with the increase of HACC concentration, whereas that on molybdenite surface increased only slightly, indicating a decreased affinity of HACC for molybdenite and a preferential attachment of HACC onto chalcopyrite surface. Noteworthily, when the concentration of HACC was 40 mg/dm³, the density of HACC adherence on chalcopyrite surface was about three times larger in comparison with that on molybdenite surface, which validated that HACC exerted a selective depression effect on chalcopyrite.

3.4. Contact angle measurements

Figure 7 shows the results of contact angle measurements. The contact angle of untreated chalcopyrite and molybdenite was 68.57° and 84.39° (D-value=15.82°), respectively. When faced with treatment by 8 mg/dm³ HACC, the contact angle of chalcopyrite decreased significantly to 32.15°, while the contact angle of molybdenite only reduced to 74.22°. It proves that HACC could selectively adsorb on chalcopyrite surface and increase its hydrophilicity, and had little effect on the hydrophilicity of

molybdenite. In combination with the results of the adsorption density of HACC on chalcopyrite and molybdenite, the selective adsorption of HACC further widened the difference in values of contact angles between the two minerals, which would facilitate the separation of these two minerals.

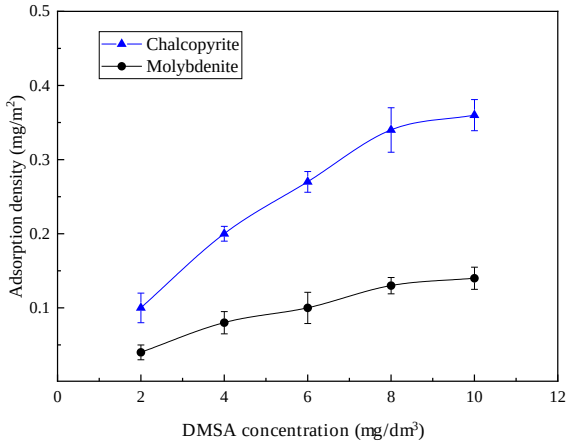

Fig. 6. Adsorption density of HACC on chalcopyrite and molybdenite

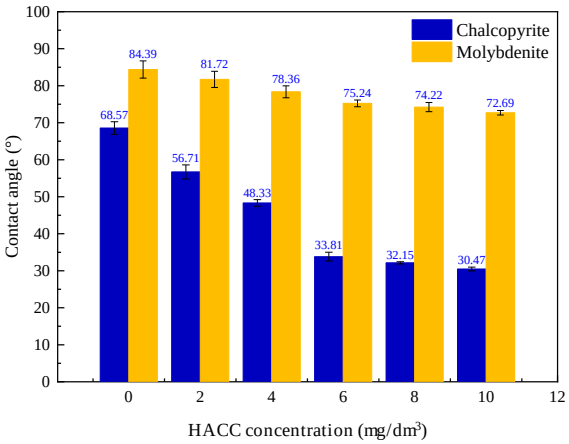

Fig. 7. Contact angle of chalcopyrite and molybdenite as a function of HACC concentration at pH around 8.0

3.5. FT-IR analysis

The high-resolution FT-IR of chalcopyrite and molybdenite before and after HACC treatment are shown in Fig. 8. In the observation range of 1250-2250 cm^{-1}, the stretching vibration absorption peak of -CH_3 was near 1383.46 cm^{-1} in the spectrum, while the two absorption peaks at 1478.18 cm^{-1} and 1653.15 cm^{-1} belonged to bending and stretching vibrations of ammonium methyl group brought about by nitrogen alkylation (Chi et al., 2007; Cai et al., 2015). After adding HACC, the absorption peak of chalcopyrite at 1401.54 cm^{-1} left shifted to 1403.58 cm^{-1}, which indicated that the -CH_3 group in HACC was adsorbed on the surface of chalcopyrite. At the same time, new absorption peaks appeared around 1645.58 cm^{-1} and 1520.14 cm^{-1}, which was caused by the large amount of ammonium methyl characteristic groups carried by HACC adsorbed on the chalcopyrite surface. There were no obvious changes in FT-IR spectra of molybdenite before and after being treated by HACC, indicating weak adsorption of HACC on the surface of molybdenite. In general, the selective adsorption of ammonium methyl groups on the chalcopyrite surface enabled efficient separation of chalcopyrite and molybdenite.

3.6. XPS analysis

In order to further determine the surface elements and their chemical states of the chalcopyrite after HACC adsorption, the XPS analysis was performed and the full spectrum of XPS is shown in Fig. 9. After the adsorption of HACC, a new peak of N 1s appeared near 400 eV in chalcopyrite surface, and

the concentration of C increased significantly, which all proved that HACC was adsorbed on the surface of chalcopyrite. Table 1 presents the relative concentration changes of main elements such as C, N, O, Fe, Cu, and S on the chalcopyrite surface before and after HACC treatment. Before the HACC adsorption, the N on the surface of chalcopyrite may be due to impurity pollution. After the adsorption of HACC, the concentrations of O, Cu, Fe, and S all decreased to varying degrees, which proved that these elements participated in the adsorption reaction. Cu element content decreased from 5.63% to 3.85%, indicating that Cu is the main metal element site for adsorption.

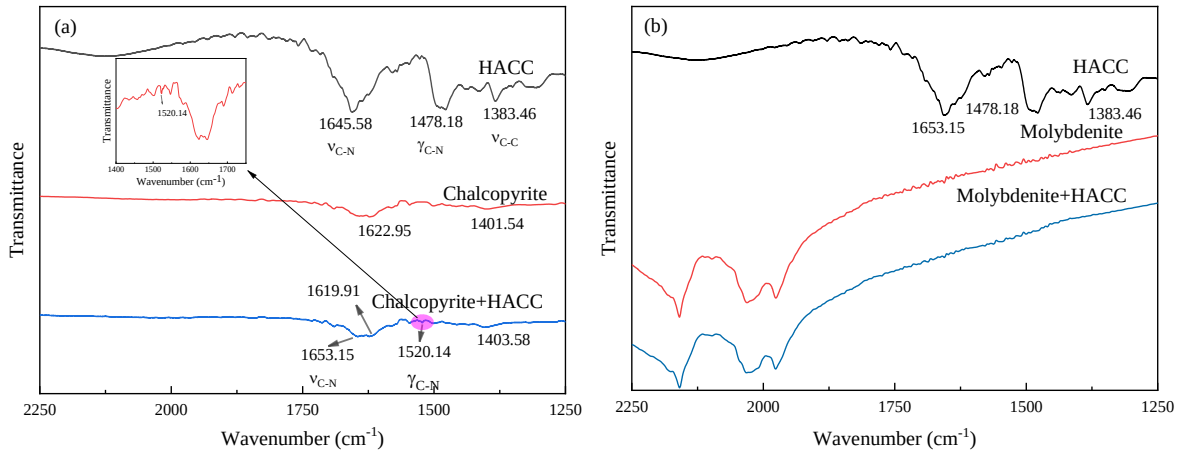

Fig. 8. FT-IR spectra (a) chalcopyrite and (b) molybdenite treated by HACC

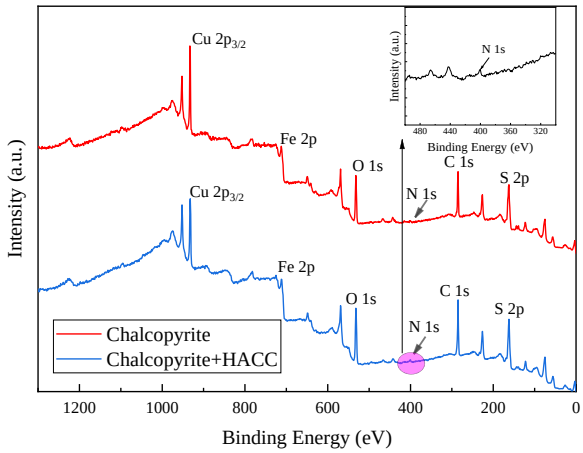

Fig. 9. Wide survey XPS spectra of HACC, chalcopyrite treated and untreated with HACC

Table 1. Changes of surface element content in chalcopyrite before and after addition of HACC (%)

Sample	C 1s	O 1s	Cu 2p	Fe 2p	S 2p	N 1s
Chalcopyrite	20.98	15.98	5.63	1.64	25.88	0.33
Chalcopyrite+HACC	34.84	12.24	3.85	1.40	16.75	0.92

The high-resolution narrow-region spectra of four elements such as C, N, Cu, and S are shown in Figs. 10, 11, 12, and 13, respectively. In Fig. 10a, the C 1s spectrum of chalcopyrite without being treated by HACC, 284.80 eV is the standard peak of C-C, and 286.68 eV belongs to the characteristic peak of C-O. After the chemical adsorption, a new characteristic peak of C-N appeared at 288.15 eV, It further illustrated that HACC is adsorbed on the surface of chalcopyrite.

The absorption peak at 400.16 eV in Fig. 11a may be due to the mixing of a small amount of N impurities in the sample preparation. After adding HACC, the N 1s absorption intensity was significantly enhanced, and there were two absorption peaks in the spectrum, of which 399.86 eV was carried by HACC itself -NH_2 group and the characteristic peak at 402.58 eV was caused by the

ammonium methyl group adsorbed on the surface of chalcopyrite, which corresponded to the results of infrared spectroscopy.

The high-resolution spectrum of Cu 2p3/2 (Fig. 12) shows that the characteristic peak of Cu 2p3/2 shifted slightly to the direction of lower binding energy after the adsorption of the reagent, which proved that HACC is physically adsorbed on the surface of chalcopyrite.

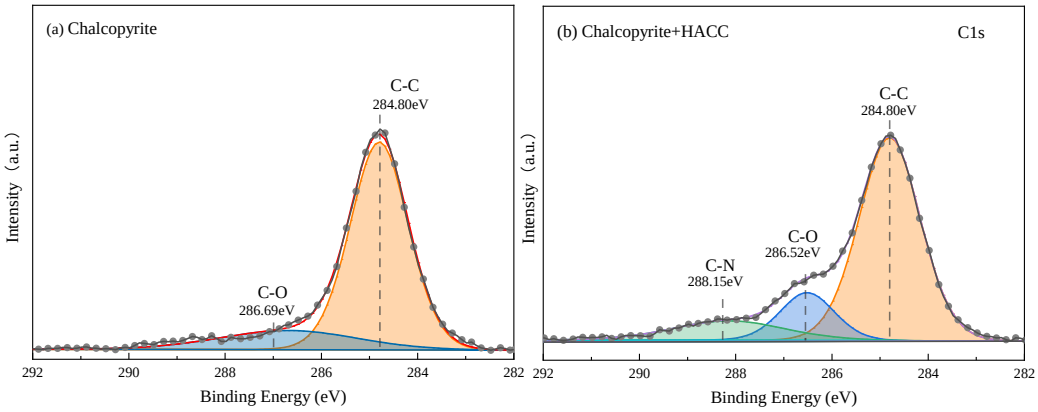

Fig. 10. The high-resolution XPS spectra of C 1s

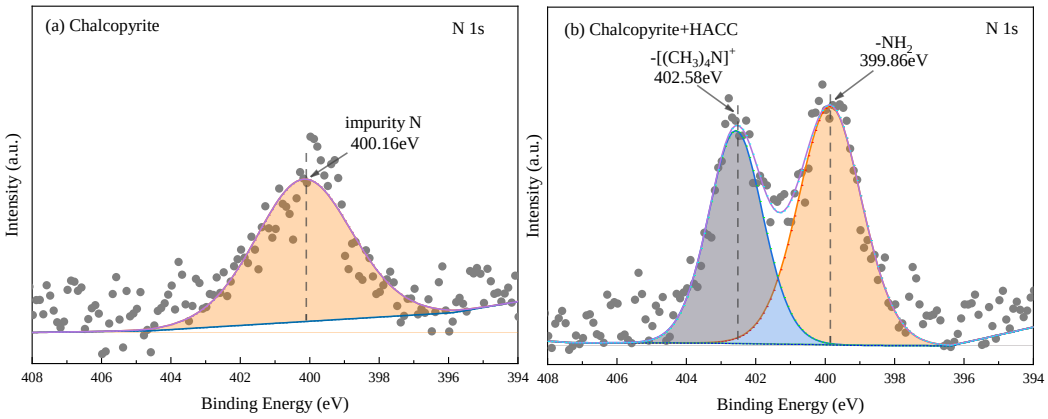

Fig. 11. The high-resolution XPS spectra of N 1s

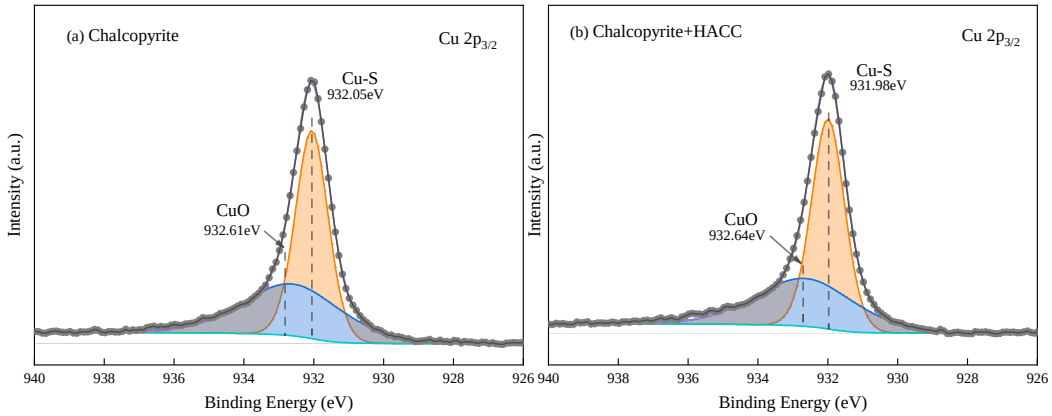

Fig. 12. The high-resolution XPS spectra of Cu 2p

In the S 2p high-resolution XPS spectrum of chalcopyrite (Fig. 13), 161.33 eV, 162.50 eV, 163.32 eV and 164.63 eV correspond to monosulfide (S^{2-}), disulfide (S_2^{2-}), polysulfide substance (S_n^{2-}) and sulfur element (S), which have been verified in previous studies (Yang et al., 2020; Zhang et al., 2020; Han et al., 2021). The peak near 168.78 eV may be the sulfate product (SO_4^{2-}), which indicated that there may

be slight oxidation on the chalcopyrite surface. The adsorption of HACC reduced the binding energy of sulfide by about 0.1 eV.

According to the comprehensive detection results, HACC adsorbs a large amount on the surface of chalcopyrite via ammonium methyl groups and mainly realized the selective depression effect on chalcopyrite by means of physical adsorption (electrostatic attraction).

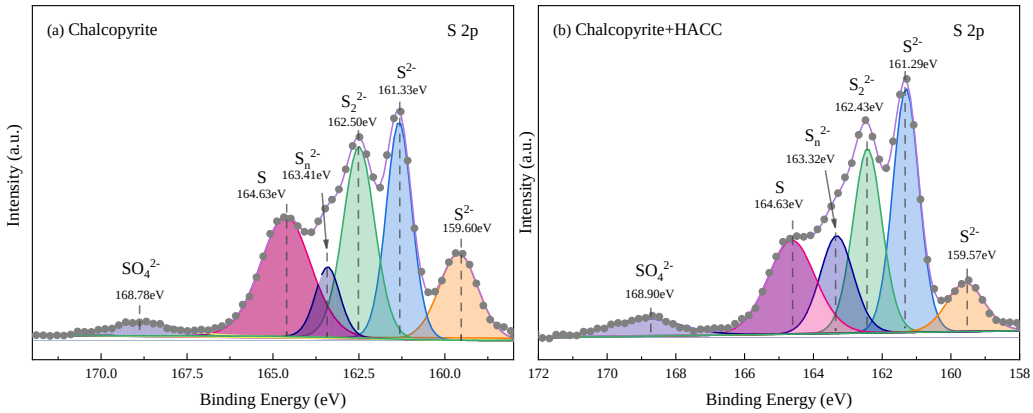

Fig. 13. The high-resolution XPS spectra of S 2p

4. Conclusions

In this study, it was discovered that hydroxypropyltrimethyl ammonium chloride chitosan (HACC) displayed depressing action on chalcopyrite for Cu-Mo sulphide ores flotation separation. The depressing performance of HACC on chalcopyrite and molybdenite was examined by means of single mineral flotation experiments, and the advertisement mechanism of HACC was researched using zeta potential, contact angle, adsorption density, FT-IR, and XPS examinations. The following conclusions could be drawn:

(1) The findings of the single-mineral flotation experiments demonstrated that HACC was able to strongly depress chalcopyrite but only had a minor effect on the floatability of molybdenite. At a concentration of 8.0 mg/dm^3 HACC and a pH of around 6.0, the recovery of chalcopyrite could be significantly minimized to as low as 5.38%. Regarding molybdenite, the recovery levels remained more than 70.0% in the whole concentration range that was investigated.

(2) The results of zeta potential, contact angle, and adsorption density measurements denoted that the selective depression of HACC on chalcopyrite resulted from the preferential attachment of HACC onto the surface of chalcopyrite, which led to a hydrophilic structure of chalcopyrite surface.

(3) The findings of FT-IR analysis suggested that the ammonium methyl groups' peaks altered after the HACC treatment of chalcopyrite, which indicated the existence of an electrostatic interaction. The XPS results revealed further evidence that the electrostatic interaction of HACC on the chalcopyrite surface was a consequence of the reaction between the primary N atom of the quaternary ammonium groups in HACC and the Cu sites on the chalcopyrite surface.

Acknowledgments

This work was supported by the financial support from the State Key Laboratory of Complex Nonferrous Metal Resources Clean Utilization (CNMRCUKF2202); Anhui Province colleges and universities (2022AH050305); State Key Laboratory of Safety and Health for Metal Mines (2022-JSKSSYS-07).

References

AL-MANHEL, A, AL-HILPHY A., NIAMAH A., 2018. *Extraction of chitosan, characterisation and its use for water purification*. Journal of the Saudi Society of Agricultural Sciences, 17(2), 186-190.

ANDREICA, B, CHENG, X, MARIN, L., 2020. *Quaternary ammonium salts of chitosan. A critical overview on the synthesis and properties generated by quaternization*. European Polymer Journal, 139, 110016.

ANSARI, A., PAWLIK, M., 2007. *Floatability of chalcopyrite and molybdenite in the presence of lignosulfonates. Part II. Hallimond tube flotation*. Minerals Engineering, 20, 609–616.

BULATOVIC, S., 2007. *Handbook of flotation reagents: Chemistry, theory and practice: Flotation of Sulfide Ores*. 1, 235–293.

CAI, J., DANG, Q., LIU C., WANG, T., FAN, B., YAN, J., XU, Y., 2015. *Preparation, characterization and antibacterial activity of O-acetyl-chitosan-N-2-hydroxypropyl trimethyl ammonium chloride*. International Journal of Biological Macromolecules, 80: 8-15.

CHEN, Y., CHEN, X., PENG, Y., 2020. *The effect of sodium hydrosulfide on molybdenite flotation as a depressant of copper sulfides*. Minerals Engineering, 148, 106203.

CHEN, X., LIU, W., WANG, L., LIU, W., SUN, W., ZHANG, N., 2023. *A novel depressant N,N-bis(phosphonomethyl)glycine for magnesite-dolomite separation and its mechanism*. Minerals Engineering, 202, 108281.

CHI, W., QIN, C., ZENG, L., LI, W., WANG, W., 2007. *Microbiocidal activity of chitosan-N-2-hydroxypropyl trimethyl ammonium chloride*. Journal of Applied Polymer Science, 103(6): 3851-3856.

GUAN, C., YIN, Z., KHOSO, S., SUN, W., HU, Y., 2018. *Performance analysis of thiocarbonohydrazide as a novel selective depressant for chalcopyrite in molybdenite-chalcopyrite separation.* Multidisciplinary Digital Publishing Institute, 8, 142.

HAN, G., WEN, S., WANG, H., FENG, Q., BAI, X., 2021. *Pyrogallic acid as depressant for flotation separation of pyrite from chalcopyrite under low-alkalinity conditions*. Separation and Purification Technology, 267: 118670.

LI, M., WEI, D., LIU, Q., LIU, W., ZHENG, J., SUN, H., 2015. *Flotation separation of copper-molybdenum sulfides using chitosan as a selective depressant*. Minerals Engineering, 83, 217-222.

LI, M., WEI, D., SHEN, Y., LIU, W., GAO, S., LIANG, G., 2015. *Selective depression effect in flotation separation of copper–molybdenum sulfides using 2,3-disulfanylbutanedioic acid*. Transactions of Nonferrous Metals Society of China, 25, 3126–3132.

LI, M., LIU, J., HU, Y., GAO, X., YUAN, Q., ZHAO, F., 2020. *Investigation of the specularite/chlorite separation using chitosan as a novel depressant by direct flotation*. Carbohydrate Polymers, 240, 116334.

LI, M., YANG, C., WU, Z., GAO, X., TONG, X., YU, X., LONG, H., 2022. *Selective depression action of taurine in flotation separation of specularite and chlorite*. Int. J. Min. Sci. Technol., 32(3), 637-644.

LIU, J., TIAN Y., AN X., LI, G., KANG, Y., 2015. *Flocculation performance and mechanism of removing pectin by n-hydroxypropyl trimethyl ammonium chloride chitosan*. Journal of Dispersion Science & Technology, 36(11), 1612-1620.

LU, L., XU, L., SHI, Q., MENG, J., LIU, R., 2022. *Microscale insights into the influence of grinding media on spodumene micro-flotation using mixed anionic/cationic collectors*. Int. J. Min. Sci. Technol., 32(1), 181-189.

MA, J., FU, K., DING, L., GUAN, Q., ZHANG, S., ZHANG, H., SHI, J., FU, X., 2017. *Flocculation performance of cationic polyacrylamide with high cationic degree in humic acid synthetic water treatment and effect of kaolin particles*. Separation & Purification Technology, 181(6), 201-212.

NAO, Y., LIU, W., CHEN, X., WANG, Z., LIU, W., SUN, W., SHEN, Y., 2023. *The role of sodium tripolyphosphate in wet grinding process of magnesite*. Colloids and Surfaces A: Physicochemical and Engineering Aspects, 668,131449.

PENG, H., WU, D., ABDALLA, M., LUO, W., JIAO, W., BIE, X., 2017. *Study of the effect of sodium sulfide as a selective depressor in the separation of chalcopyrite and molybdenite*. Minerals, 7, 51.

POPERECHNIKOVA, O.Y., FILIPPOV, L.O., SHUMSKAYA, E.N., FILIPPOVA, I.V., 2017. *Intensification of the reverse cationic flotation of hematite ores with optimization of process and hydrodynamic parameters of flotation cell*. Journal of Physics: Conference Series, 879(1), 012016.

RINAUDO, M., 2007. *Chitin and chitosan: properties and applications*. Cheminform, 31(7), 603-632.

SUYANTARA, G., HIRAJIMA, T., MIKI, H., SASAKI, K., YAMANE, M., TAKIDA, E., KUROIWA, S., IMAIZUMI, Y., 2018. *Effect of Fenton-like oxidation reagent on hydrophobicity and floatability of chalcopyrite and molybdenite*. Colloids and Surfaces A: Physicochemical and Engineering Aspects, 554, 34–48.

TRIFFETT, B., VELOO, C., ADAIR, B., BRADSHAW, D., 2008. *An investigation of the factors affecting the recovery of molybdenite in the Kennecott Utah Copper bulk flotation circuit*. Minerals Engineering, 21(12-14), 832-840.

WEI, Z., LI, Y., HUANG L., 2021. *New insight into the anisotropic property and wettability of molybdenite: A DFT study*, Minerals Engineering. 170, 107058.

YAN, H., YANG, B., ZENG, M., HUANG, P., TENG, A., 2020. *Selective flotation of Cu-Mo sulfides using xanthan gum as a novel depressant*. Minerals Engineering, 156, 106486.

YANG, B., YAN, H., ZENG, M., HUANG, P., JIA, F., TENG, A., 2020. *A novel copper depressant for selective flotation of chalcopyrite and molybdenite*. Minerals Engineering, 151, 106309.

YIN, W., ZHANG, L., XIE, F., 2010. *Flotation of Xinhua molybdenite using sodium sulfide as modifier*. Transactions of Nonferrous Metals Society of China, 20(4), 702–706.

YIN, Z., SUN, W., HU, Y., ZHAI, J., GUAN, Q., 2017. *Evaluation of the replacement of NaCN with depressant mixtures in the separation of copper–molybdenum sulphide ore by flotation*. Separation and Purification Technology, 173, 9-16.

YIN, Z., CHEN, S., XU, Z., ZHANG, C., HE, J., ZOU, J., CHEN, D., SUN, W., 2020. *Flotation separation of molybdenite from chalcopyrite using an environmentally efficient depressant L-cysteine and its adsorption mechanism*. Minerals Engineering, 156, 106438.

YUAN, D., CADIEN, K., LIU, Q., ZENG, H., 2019. *Selective separation of copper-molybdenum sulfides using humic acids*. Minerals Engineering, 133, 43–46.

ZHANG, X., LU, L., CAO, Y., YANG, J., CHE, W., LIU, J., 2020. *The flotation separation of molybdenite from chalcopyrite using a polymer depressant and insights to its adsorption mechanism*. Chemical Engineering Journal, 395, 125137.

ZENG, G., OU L., ZHANG W., ZHU, Y., 2020. *Effects of sodium alginate on the flotation separation of molybdenite from chalcopyrite using kerosene as collector*. Frontiers in Chemistry, 8, 242.

ZHONG, C., FENG, B., WANG, H., CHEN, Y., GUO, M., 2021. *The depression behavior and mechanism of tragacanth gum on chalcopyrite during Cu-Mo flotation separation.* Advanced Powder Technology, 32, 2712–2719.